PROCEEDINGS OF SPIE

SPIEDigitalLibrary.org/conference-proceedings-of-spie

A fast 512-element ring array photoacoustic imaging system for small animals

John Gamelin, Anastasios Maurudis, Andres Aguirre, Fei Huang, Puyun Guo, et al.

John Gamelin, Anastasios Maurudis, Andres Aguirre, Fei Huang, Puyun Guo, Lihong V. Wang, Quing Zhu, "A fast 512-element ring array photoacoustic imaging system for small animals," Proc. SPIE 7177, Photons Plus Ultrasound: Imaging and Sensing 2009, 71770B (24 February 2009); doi: 10.1117/12.812406

SPIE.

Event: SPIE BiOS, 2009, San Jose, California, United States

A fast 512-element ring array photoacoustic imaging system for small animals

John Gamelin, Anastasios Maurudis, Andres Aguirre, Fei Huang, Puyun Guo, Lihong V. Wang*, and Quing Zhu

University of Connecticut, Biomedical Ultrasound and Optical Imaging Group, Storrs, CT 06269
* Washington University in St. Louis, Dept. of Biomedical Engineering, St. Louis, MO 63130-4899

ABSTRACT

A 512-element photoacoustic tomography system for small animal imaging using a ring ultrasound array has been developed. The system features a 5 MHz piezocomposite transducer array formed into a complete circular aperture. Custom receiver electronics consisting of dedicated preamplifiers, 8:1 multiplexed post-amplifiers, and a 64-channel data acquisition module provide full tomographic imaging at up to 8 frames/second. We present details of the system design along with characterization results of the resolution, imaging volume, and sensitivity. Small animal imaging performance is demonstrated through images of mice brain vasculature at different depths and real-time spectroscopic scans. This system enables real-time tomographic imaging for functional photoacoustic studies for the first time.

Keywords: Photoacoustic tomography, real-time imaging, reconstruction, backprojection

1. INTRODUCTION

Photoacoustic tomography (PAT) has emerged as a promising biomedical imaging modality due to its ability to produce ultrasound-resolution images using intrinsic optical contrast[1]. To date, however, full tomographic imaging has been limited to static conditions due to the long imaging times (minutes to hours) accompanying scanning of single element transducers or limited-view linear transducer arrays. Many dynamic functional and *in vivo* studies require acquisition rates on the order of seconds to milliseconds such as monitoring the uptake of targeted contrast agents or investigating physiological responses to external stimuli as in functional brain imaging. In addition, control of animal physiological parameters, motion, and anesthesia during these extended measurement periods can present significant challenges for obtaining quality images.

We previously demonstrated a 128-channel photoacoustic imaging system based upon a curved ultrasound array that captured a 90-degree field of view in less than one second, but required sample rotation for complete tomographic imaging[2]. The increased scan time (15-30 seconds) for tomographic imaging and the registration errors associated with

Photons Plus Ultrasound: Imaging and Sensing 2009, edited by Alexander A. Oraevsky, Lihong V. Wang,
Proc. of SPIE Vol. 7177, 71770B · © 2009 SPIE · CCC code: 1605-7422/09/$18 · doi: 10.1117/12.812406

the mechanical rotation prevented imaging of short-duration physiological responses and introduced some distortion of the high-resolution (< 200 μm) images.

In this paper, we report development and small animal imaging results of a second-generation system employing a 512-channel full-ring configuration. By eliminating the speed and registration issues due to mechanical scanning and increasing the parallel receiver electronics, the system achieves, for the first time, a complete two-dimensional tomographic imaging in less than one second. The organization of this paper is as follows. We first present details of the system design and highlight characterization results of the system performance in terms of resolution and imaging volume. The capabilities of the system are then explored through *ex vivo* and *in vivo* imaging of mouse brain vasculature.

2. SYSTEM DESIGN

Figure 1 presents a block diagram of the experimental set-up and architecture of our 512-channel photoacoustic tomography imaging system. A Ti:Sapphire (Symphotics TII, LS-2134) laser optically pumped with a Q-switched Nd:YAG laser (Symphotics-TII, LS-2122) generates 8-12 ns pulses at 15 Hz with a wavelength tunable from 700-950 nm. The beam is expanded with a Galilean telescope assembly and subsequently diverged with either a plano-concave lens or homogenized by a circular profile engineered diffuser (ED1-S20, ThorLabs, Newton, NJ). The laser beam is positioned at the center of the transducer and strikes the stage orthogonal to the imaging plane of the transducer for maximum uniformity.

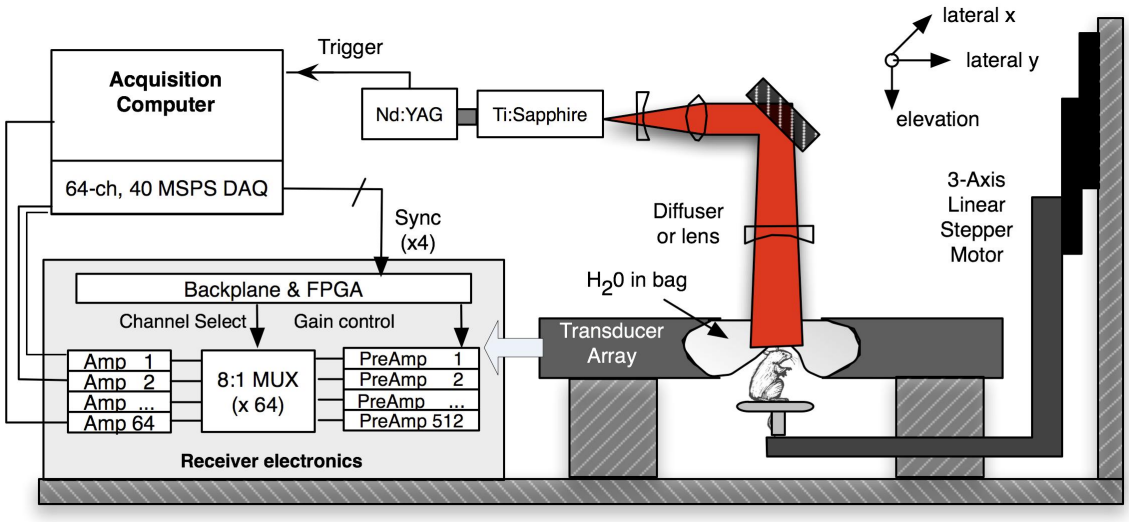

Figure 1. Block diagram of system.

The transducer array, custom manufactured by Imasonic (Besancon, France), consists of 512 elements arranged along a closed curved aperture with a diameter of 50 mm. Internally, the transducer contains four 90-degree segments positioned precisely with minimal kerfs between adjacent sections. The 1,3-piezocomposite array features a center frequency of 5.1 MHz and a photoacoustic bandwidth greater than 100%. To achieve wide directivity of individual elements, the elements were chosen to have a lateral pitch of approximately one wavelength (0.3 mm) at the central frequency. Each element is directly shaped in elevation to produce a mechanical focal depth of 19 mm without the loss and acoustic aberrations of external lenses. The combined focal points of all elements form a ring around the central imaging region with a diameter of 1.2 cm. Lateral electronic scanning is employed within the elevation focal plane.

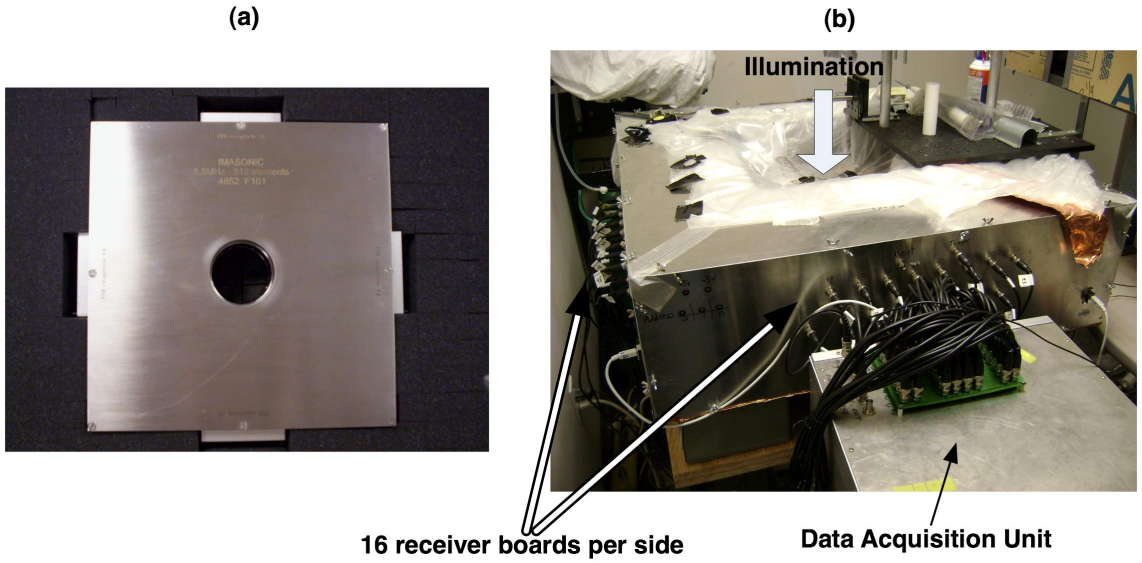

Figure 2. (a) Photograph of transducer. (b) Photograph of system illustrating front-end electronics and data acquisition unit.

Custom front-end electronics and matching data acquisition system were designed and constructed in our lab because of the large number of channels (Figure 2b). The electronics are distributed among 64 boards, each servicing 8 transducer elements, arranged in four quadrants surrounding the transducer. For high sensitivity and immunity to external interference, all connections to the transducer elements employ coaxial cables of less than 12 inches length. A three-axis linear stepper motor drive unit, located beneath the transducer chassis, provides full control of sample position within the 45 mm open transducer aperture. In order to facilitate water coupling, an integral flexible plastic bag was secured to the periphery of the metallic base of the transducer block. The sample platform, connected to the stepper motor stages, penetrated through the clear bag with a watertight coupling.

As depicted in Figure 1, the laser Q-switch provides the master timing for the system and triggers the acquisition unit. Upon absorption of the laser pulse, 512 dedicated low-noise, 20dB gain preamplifiers amplify the transient photoacoustic waves measured around the sample. To reduce the number of acquisition channels, sixty-four multiplexers select one of eight channels and forward the outputs to low-noise second-stage amplifiers. The gain of the post-amplifiers can be electronically controlled from 20 dB to 100 dB. Further details of the front-end electronics have been reported elsewhere [2].

In the data acquisition module, the 64 output signals are filtered by 15 MHz anti-aliasing bandpass filters (Mini-Circuits, New York, NY) and digitized by parallel 40 MHz A/D chips with 10 bits precision**.** The data from each acquisition is DMA-transferred to RAM and accumulated over the experimental duration to maximize the imaging speed. The acquisition computer subsequently transfers the measurement data to disk for post-processing. With the 8:1 multiplexing, eight laser firings are required to generate a complete 512-channel capture. Data setup and transfer for results of a single acquisition can be performed at up to 8 Hz, leading to a maximum rate of 1 frame/second with full tomographic resolution. Using sliding acquisition techniques, imaging at the 8 frame/sec acquisition rate, has been demonstrated.

3. CHARACTERIZATION RESULTS

The frequency response of the transducer was evaluated by measuring the photoacoustic response from the absorbing transducer face using weakly scattered light. As illustrated in Figure 3 for a typical element, the peak response frequency is approximately 5 MHz with a -6 dB bandwidth extending from 2.7 to 7.9 MHz (100%). Because of the large number of elements and construction from four independent 128-channel subunits, some variation in performance is expected throughout the array. The uniformity was directly measured by illuminating the full ring with light scattered from the tip of a 500-micron pencil lead positioned at the center of the ring to generate an isotropic excitation signal.

Figure 4a depicts the measured time response of the signal produced from absorption on the transducer surface for all elements. The delay and phase characteristics demonstrate high uniformity, but the amplitudes depend upon location within the transducer aperture. Figure 4b plots the envelope amplitude of the response as a function of element number. Discontinuities at 128-element boundaries, expected due to the discrete construction, are observed. The total variation across elements is approximately 12 dB. The manufacturer, using the pulse-echo response from a cylindrical target, measured similar response variation curves. The sensitivity and time response of the individual elements was deconvolved from the measured data using Wiener deconvolution techniques[3].

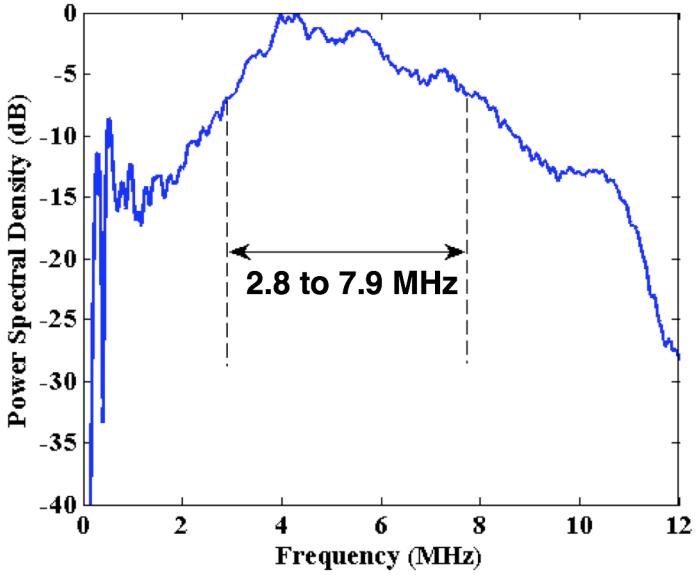

Figure 3. Measured photoacoustic frequency response of typical transducer element.

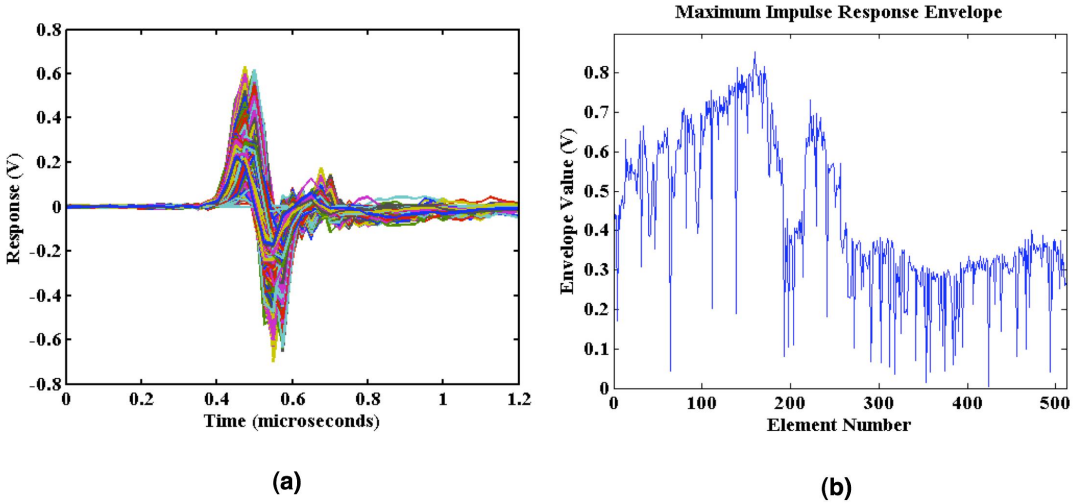

Figure 4. (a) Measured transient photoacoustic response of absorption from transducer surface for all elements. (b) Corresponding envelope amplitude of photoacoustic response versus element number.

The resolution and imaging volume of the system were investigated by scanning of an 80-micron black thread with a length of 1.5 mm (in the elevation direction) radially from the center of the array. The peak value and lateral/radial resolutions were estimated from the resulting photoacoustic images obtained using a backprojection algorithm. Figure 5 depicts the measured resolutions as a function of the distance from the center of the

transducer. For comparison, the predictions of the analytical theory of Xu and Wang[4] are also plotted. The theoretical calculations account for the target diameter, the limited frequency response of the transducer, and the spatial resolution contributions. As expected, the radial resolution is independent of imaging position. In contrast, the lateral resolution increases almost linearly with distance, theoretically reaching the transducer element size at the periphery of the ring.

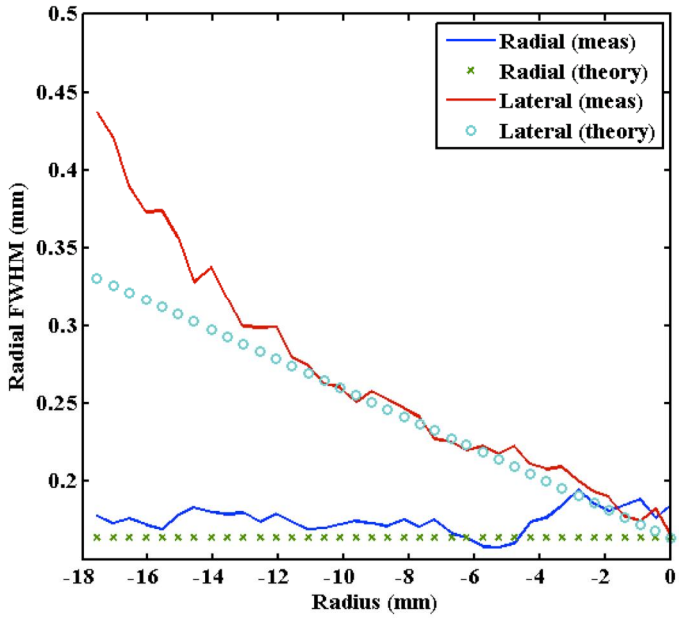

Figure 5. Measured lateral and radial resolution vs. radius. Theoretical predictions are presented for comparison. The 80-micron thread diameter is not subtracted from these results.

Nonlinear increases in the lateral resolution were observed for locations beyond about 10 mm from the center. We believe this deviation is due to the combination of element directivity and elevation focus effects that both act to limit the number of elements that effectively contribute to image formation near the periphery. In practice, this deviation is not significant as the sensitivity falls off rapidly in the same regions because of the same physical mechanisms. Within the defined region, the system obtains a resolution of better than 200 micron after subtracting the 80-micron target diameter.

Figure 6 plots the measured relative sensitivity as a function of radial location along with results of simulations using the Field II ultrasound simulation program[5]. The response peaks near the elevation focus and decreases in both directions away from this radius. Because of the nearly equal contributions of all elements close to the center of the imaging region, the sensitivity drop-off is weaker in this direction. Defining the imaging region by a response within 6 dB of the peak, the imaging region represents a central region of approximately 2 cm diameter. In the perpendicular direction, the simulations predict a "slice" thickness of 0.6 (elevation focus) to 2.5 mm (center). The wide-but-thin,

disk-shaped imaging volume is well matched for the intended design purpose of three-dimensional tomographic imaging of mice and rat brain vasculature.

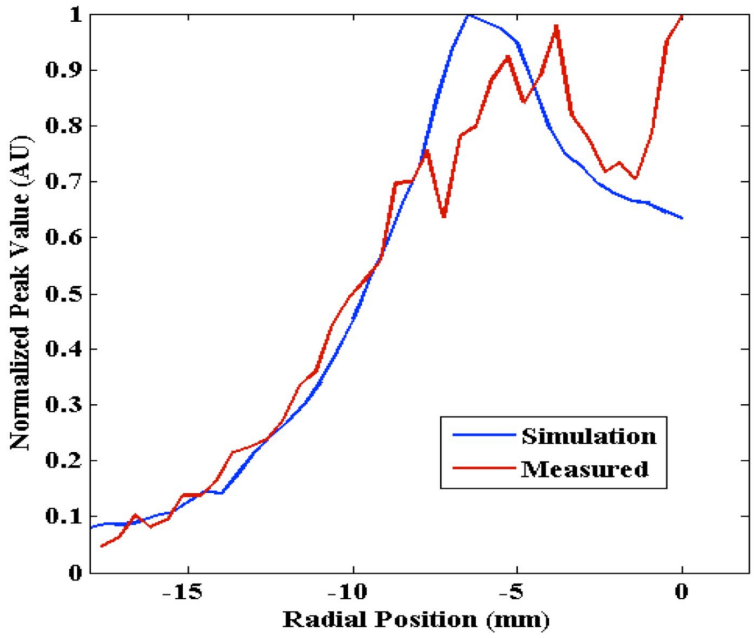

Figure 6. Comparison of measured and simulated response vs. radius for the transducer array.

4. MOUSE BRAIN IMAGING

The ability of the system to perform depth-discriminated imaging was evaluated with vascular imaging of rodent brains. *Ex vivo* experiments were performed with freshly sacrificed 50 g white rats with intact skull and skin (hair removed). The rats were acquired from the University of Connecticut Office of Animal Research and were euthanized in accordance with procedures of the University Institutional Animal Care and Use Committee as well as the National Institutes of Health. The rats were mounted in a 1.5" diameter PVC pipe with the skull level with the imaging plane. Full tomographic images were obtained at depths up to 6 mm with incident fluence levels were maintained below 15 mJ/cm^2.

Figure 7 presents images obtained at depths corresponding to approximately 1 and 5 mm below the top of the skull. For comparison, open-skull photograph from dorsal and basal surfaces are included. These surfaces are not coincident with the imaging planes but serve to identify feature correspondences. Near the brain surface, the superior sagittal and cerebral veins including branches are visible in addition to the top surfaces of the

eyes. At the deeper cross-section, basalar veins and the middle cerebral artery can be observed along with ringed features near the brain stalk not visible in the photographs.

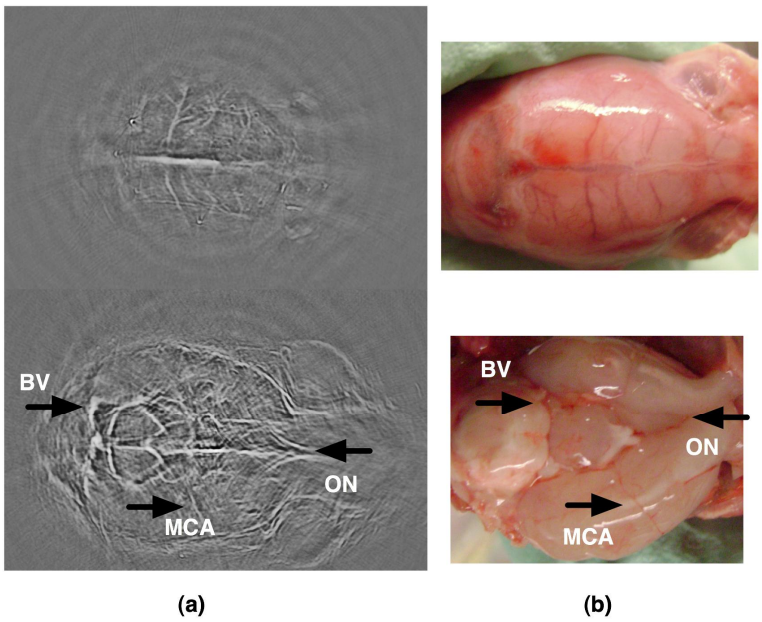

Figure 7. (a) Photoacoustic images at 1 and 5 mm below skin surface. (b) Open-skull photographs of top and basal surfaces of brain. Legend: BV=Basalar vein, MCA=Mid-cerebral artery, ON=optic nerve.

Real-time performance was demonstrated through *in vivo* spectroscopic imaging experiments on 4-6 week old female, CD-1 mice. All experiments were carried out under a protocol approved by the University of Connecticut Institutional Animal Care and Use Committee. The mice were mounted upright in white PVC tubing with the skull level to the lateral imaging planes. An isoflurane (2%) gas system (VetEquip, Pleasonton, CA) delivered anesthesia through a custom miniaturized polyethylene mask to fit within the 44 mm aperture of the transducer. Prior to imaging, hair was removed using a depilitating cream. The wavelength was manually scanned from 710 to 900 nm over a 30-second interval and the photoacoustic images obtained at 8 frames/sec using a sliding time-window technique in which the most recent data for each element was used for imaging.

.

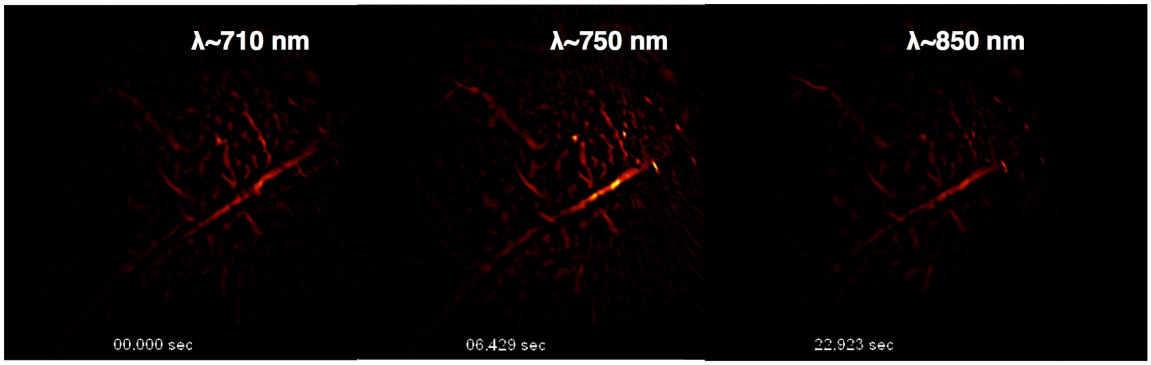

Figure 8. Still photoacoustic images from t=0, 6.4, and 22.9 seconds for a real-time, in vivo spectroscopic scan of mouse brain vasculature from 710 to 900 nm over a 30-second interval.

Figure 8 depicts frames from the image sequence corresponding to wavelengths of 710, 750, and 850 nm at corresponding times of 0, 6.4 and 22.9 seconds. Fewer features were resolved in this sequence because of the presence of the bag and breathing apparatus that introduced spurious reflections, reduced the number of elements receiving signal, and increased losses. Nevertheless, the images demonstrate the potential of the system to provide real-time, *in vivo* spectroscopic or functional imaging at rates approaching the repetition rate of the laser.

5. CONCLUSION

We have presented results from a 512-channel full tomographic photoacoustic system designed for small animals. The system features a high resolution of better than 200 microns over a disk-shaped volume of approximately 2 cm diameter and thickness of 0.6 to 2.5mm. Images of rat and mouse brain vasculature demonstrated the capability to perform depth-resolved imaging with a frame rate of 1 to 8 frame/sec. This real-time tomographic imaging ability enables, for the first time, dynamic functional and spectroscopic *in vivo* studies with small animals, fulfilling a long-sought promise of photoacoustic imaging.

6. ACKNOWLEDGMENTS

We acknowledge partial support from NIH grants NIH R01EB002136 and the Patrick and Catherine Weldon Donaghue Research Foundation. The authors can be contacted at via e-mail at zhu@engr.uconn.edu.

7. REFERENCES

[1]M. H. Xu & L. H. V. Wang, "Photoacoustic imaging in biomedicine," Review of Scientific Instruments **77(4),** 041101 (2006).

[2]J. Gamelin, A. Aguirre, A. Maurudis, F. Huang, D. Castillo, L. V. Wang et al., "Curved array photoacoustic tomographic system for small animal imaging," J Biomed Opt **13(2),** 024007 (2008).

[3]Gonzales, R., Woods, R., & Eddins, S., [Digital Image Processing Using Matlab], Prentice Hall, (2003).

[4]M. Xu & L. V. Wang, "Analytic explanation of spatial resolution related to bandwidth and detector aperture size in thermoacoustic or photoacoustic reconstruction," Phys Rev E Stat Nonlin Soft Matter Phys **67(5 Pt 2),** 056605 (2003).

[5]J. A. Jensen, "Field: A program for simulating ultrasound systems," Medical & Biological Engineering & Computing **34 (1-1),** 351-353 (1996).